Indian Journal of Pure & Applied Physics
Vol. 55, November 2017, pp. 806-812

Experimental and neural network approach to effective electrical conductivity of carbon nanotubes dispersed chiral nematic liquid crystals

Rishi Kumar[a,b], R P Singh[c]*, Manju Middha[a] & K K Raina[a]

[a]Materials Research Laboratory, School of Physics and Materials Science, Thapar University, Patiala 147 004, India

[b]Department of Science,Guru Nanak College, Budhlada 151 502, India

[c]Department of Physics, Government Rajindra College, Bathinda 151 001, India

Received 1 September 2016; accepted 12 June 2017

Single walled carbon nanotubes (SWCNT's) doped cholesteric liquid crystal composite has been prepared and characterized for their electrical responses. Also theoretically, an artificial neural network (ANN) approach has been trained for predicting the effective electrical conductivity of these composites. The ANN models are based on a feedforward backpropagation (FFBP) network with such training functions as the adaptive learning rate (GDX), gradient descent with adaptive learning rate (GDA), gradient descent (GD), conjugates gradient with Powell-Beale restarts (CGB), one-step secant (OSS), and Levenberg–Marquardt (LM), and training algorithms run at the uniform threshold transfer functions-Tangent sigmoid (TANSIG) and pure linear (PURELIN) for 1000 epochs. Our modeling confirms that the expected effective electrical conductivity by different training functions of ANN is in higher agreement with the experimental results of SWCNT doped CLC composites.

Keywords: Single walled carbon nano tubes (SWCNTs), Electrical conductivity, Liquid crystals, Artificial neural network, Electro-optic switching

1 Introduction

In recent decades, Liquid crystals (LCs) have received much attention onto dispersed nanomaterials, such as carbon nanotubes (CNT's), carbon dots, quantum dots (QD's), nanorods and various shaped nano colloids for their ability to transfer their long range orientational order[1-5]. CNT's are usually well characterized for their extremely high anisotropy and electrical conductivity. So the dispersion of CNT's into liquid crystal provides a fascinating composite system that involves an anisotropic colloidal dispersion in an anisotropic medium material with improved intrinsic electrical conductivity[6,7]. Novel electro-optic liquid crystal devices based on this novel material have been developed in the display market where the control of alignment of CNTs is highly demanded[8-12]. It was earlier reported that the alignment of CNTs can easily drive by LC reorientations under an external stimulus. Various research groups over the globe focused on the control of alignment of CNTs and improved electrical behavior of composite materials[10-14]. It was predicted experimentally that the surface anchoring along with a binding energy of about ~ 2 eV for π-π electron stacking between chiral nematic and CNT's is responsible for a strong interaction in SWCNT's doped chiral nematic liquid crystal and hence enhanced electrical conductivity.

Yet lots of experimental evidence has been reported on the improved behavior of electrical conductivity of CNT doped liquid crystals, but the prediction of electrical conductivity of these composites using an algorithm is still challenging in the field of ongoing research in liquid crystals. An artificial neural network (ANN) seems a potential candidate to simulate electrical properties of a variety of complex liquid crystals.

Since the early 1990s, ANNs have been of interest for many researchers and they applied it successfully to almost every problem in geotechnical and in thermal engineering. ANNs are thus well suited for modeling the complex behavior of polymer composite. Recently, Therdthai *et al.*[15] measured the electrical conductivity of recombined milk by artificial neural network (ANN). Ali *et al.*[16] predicted the electrical conductivities of ternary systems involving ionic liquids by the applicability of artificial neural network. In the last few years, many researchers[17-20] used artificial neural network approach to predict the conductivity of different composites.

*Corresponding author (E-mail: rishikumar.phd@gmail.com)

Presently in this paper, we have tried to set up a nonlinear relationship between the experimentally calculated electric conductivity and theoretically predicted value during the training process of ANN network. In reality, SWCNT doped cholesteric liquid crystal forms a complex inner structure. Therefore, its complex geometry encountered large difference in the electrical conductivity along with its constituents. It makes very tedious task to predict the effective electrical conductivity of SWCNT doped CLC composites. For this reason we have developed an artificial neural network to find out the effective electrical conductivity of SWCNT doped CLC samples.

2 Experimental Details

A room temperature nematic liquid crystal ZLI-4151 (E. Merck, UK) and an active chiral dopant CB15 (E. Merck, Dermstadt, Germany) was used to make chiral nematic liquid crystal mixture. A series of SWCNT doped chiral nematic mixtures was formed by dispersion of Octadecylamine (ODA)-functionalized SWCNTs [M/s Sigma Aldrich], having diameter ≈ 2–10 nm and length ≈ 0.5–2 μm with doping concentrations 0.05, 0.10, 0.15, 0.20, 0.25, 0.30, 0.35 and 0.4 weight % into chiral nematic mixture. The ODA Functionalization of SWCNT's was confirmed with the help of Fourier transform infrared (FTIR) spectra in ethanol (Fig. 1). The spectra were studied by using IR spectrophotometer [Model-Perkin Elmer BX–II; Waltham, MA, USA]. The dip correspond to 1046.49 cm^{-1} confirms C–N stretching; whereas dip correspond to 1381.76 cm^{-1} confirms simple bending vibrations of C–H bonds. The confirmation of asymmetric and symmetric vibrations of C-H bond was given by dips at 2908.74 and 2842.10 cm^{-1}. The signature of O-H stretch of vibration was confirmed by the broad dip at 3439.96 cm^{-1} whereas the dip at 1589.99 cm^{-1} corresponds to C=O stretch, this clearly indicate introduction of long-chain ODA to SWCNTs. Again the size Octadecylamine (ODA)-functionalized SWCNTs has been confirmed of the order ≈ 2–10 nm with TEM micrograph (shown in Fig. 1(b)).

These composite mixtures of ODA functionalized SWCNT's doped CLC were sandwiched into the 5 μm thin antiparllel planer aligned indium tin oxide (ITO) coated glass substrates. Then cells were sealed by Norland optical adhesive epoxy glue. Electrical contacts with conducing ITO substrate were made by using indium solder to record the electrical responses of SWCNT doped chiral nematic cells. The dielectric responses of these were investigated by recording capacitance in frequency range 50 Hz to 1 MHz with Fluke LCR bridge (Model PM6306) and further effective electrical conductivity was calculated experimentally with the help of complex permittivity.

3 Theoretical Approach of Neural Network

ANNs are electronic models that are based on the brain's neural structure. The experience are helpful for the brain to learn. This brain modeling also promises a less technical way to the development machine solutions. The ANNs are new approach to computing the data and also provide a more graceful degradation during system overload. In the computing industry the biologically inspired methods play an important role for computing. Animal brains are capable of functions that are not possible by computers. Computers performs complex math. But computers have not capable recognizing simple patterns and much less efficiency those patterns of the past into actions of the future.

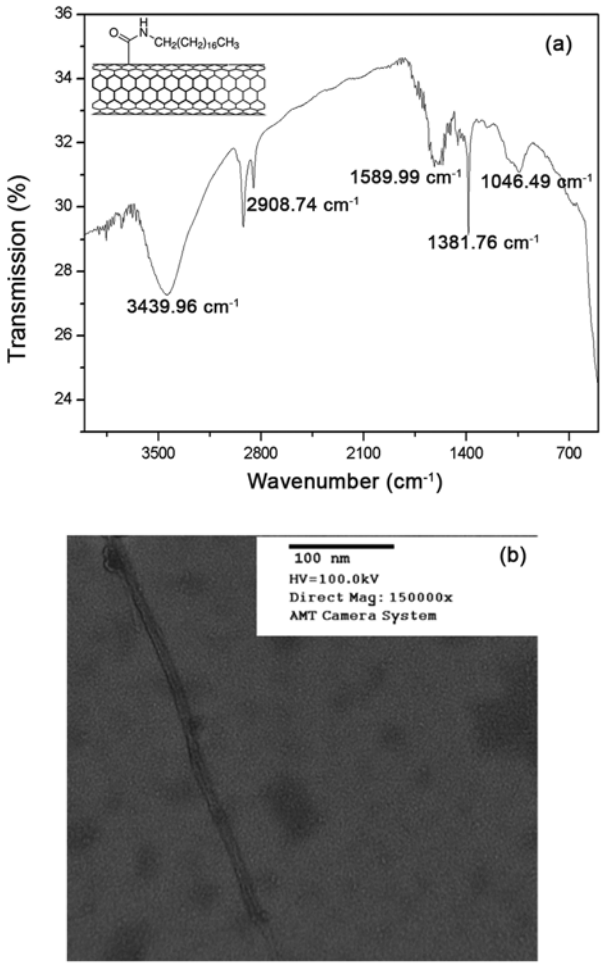

Fig. 1 — (a) FTIR spectra and (b) TEM micrograph of ODA functionalized SWCNTs.

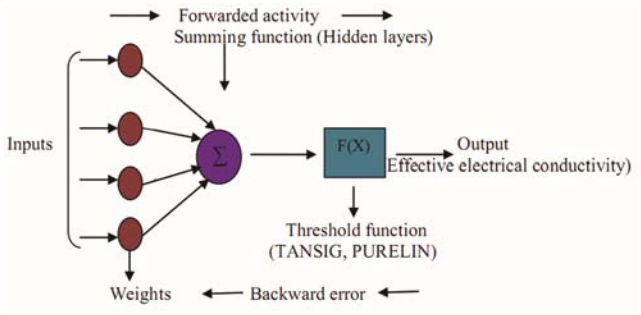

Fig. 2 — Three layer artificial neural network.

It should also be reiterated here that the designed models are "statistical" models, i.e., they are not based on any physical complex theory. Because of this, the highest precision of the predictions is expected when there are immense numbers of input data for the materials.

In a simplified mathematical model (Fig. 2) of the neurons, the effects of the synapses are represented by connection weights that modulate the effect of the associated input signals, and the non-linear characteristic exhibited by neurons is represented by a transfer function. The neuron impulse is then computed as the weighted sum of the input signals, transformed by the transfer function[21]. The learning capability of an artificial neuron is achieved by adjusting the weights in accordance to the chosen learning algorithm. It stimulates the results among homologous series of ANN algorithms without need for theoretical formulas. It is based on feed-forward back propagation (FFBP) network with training functions: adaptive learning rate (GDX), gradient descent with adaptive learning rate (GDA), gradient descent (GD), conjugates gradient with Powell-Beale restarts (CGB), one-step secant (OSS), and Levenberg–Marquardt (LM). Training algorithm for neurons and hidden layers for given different FFBP networks for 1000 epochs runs at the uniform threshold tangent sigmoid-pure linear transfer function. During training the network, calculations were carried out from input of network toward output and error was then propagated to prior layers. Output calculations were conducted layer to layer so that the output of each layer was the input of next one.

Rumelhart *et al.*[22] presented the neural network model as a three-layer feed forward neural network. Each layer is fully connected to the succeeding layer through the connection weights (Fig. 2). The electrical conductivity and volume fractions of the constituents respectively are the input parameters to predict the effective electrical conductivity of SWCNT's doped chiral nematic liquid crystals. The activation (threshold) functions used for the network are:

(i) Pure linear transfer function (PURELIN):

$$Y_j = AX_j \qquad \ldots (1)$$

and (ii) A tangent sigmoid trandfer function (TANSIG), which is a non-linear function:

$$Y_j = \frac{2}{\left(1+\exp\left(-2X_j\right)\right)-1} \qquad \ldots (2)$$

The following relation is used for the mean square error (E_{MSE}), which can minimize the training error:

$$E_{\text{MSE}} = \sum_{k=1}^{N}\left(A_k - T_k\right)^2 \qquad \ldots (3)$$

where A_k and T_k are the network (actual) and target outputs at k^{th} output unit; N is the number of output neurons. To find a set of weights that minimizes this function, a gradient descent method was implemented. The weight change is proportional to the negative of the derivative of the error with respect to each weight. This can be expressed as:

$$\Delta w \propto \frac{-\partial E_{\text{MSE}}}{\partial w} \qquad \ldots (4)$$

Essentially, the determination of the weight change is a recursive process, which starts with the output units. For a weight that is connected to a unit in the output layer, its change is based on the error of the output unit. It is given by:

$$\Delta w_{kj} \propto A_k\left(1-A_k\right)\left(T_k - A_k\right)A_j = \delta_k A_j \qquad \ldots (5)$$

where w_{kj} is the weight of the connection between the k^{th} and j^{th} unit. δ_k referred as the error signal in the k^{th} output unit. The output error signals are then back propagated to the units in the hidden layer. The change of the weight in the hidden layer is determined by the relation:

$$\Delta w_{ji} \propto A_j\left(1-A_j\right)\sum_k \delta_k w_{kj} A_i = \delta_j A_i \qquad \ldots (6)$$

In order to increase the speed of the training procedure without any oscillations, the adaptive learning rate and momentum are used during the training process. The Eqs (5) and (6) are then reformatted as follows:

$$\Delta w_{kj}(n) = \xi \delta_k A_j + \alpha \Delta w_{kj}(n-1) \quad \ldots (7)$$

$$\Delta w_{ji}(n) = \xi \delta_j A_i + \alpha \Delta w_{ji}(n-1) \quad \ldots (8)$$

where n, ξ and α represent the training epoch number, learning rate and the momentum, respectively. The momentum allows the previous weight change, which has a continuing influence on the current weight change. The gradient correlation of the present weight error derivatives with the previous weight error derivatives indicates whether the gradient is staying relatively stable or shifting. According to it, the learning rate and momentum automatically change the number of epochs and kept as large as possible. The following function is the mean square error which minimized the training error:

$$E = \sum_{k=1}^{M} \sum_{i=1}^{N} (S_{ik} - T_{ik})^2 \quad \ldots (9)$$

where E is the mean square error, S_{ik} is the network output in i^{th} neuron and k^{th} pattern, T_{ik} is the target output at i^{th} neuron and k^{th} pattern; N is the number of output neurons and M is the number of training patterns. Thus, the outputs are determined for each epoch, the mean square error is then calculated and the weights updated till a user specified epoch goal is reached successfully.

4 Results and Discussion

4.1 Electro-optic switching analysis

Figure 3 depicts the electrical switching behavior of SWCNTs doped and undoped chiral nematic liquid crystals. The morphology in "Switch OFF and Switch ON state" was investigated at 100X magnification through crossed polarizers in Carl Zeiss polarizing optical microscope (Model-Scope A1) interfaced with charge coupled device (CCD) detector. At E=0 V/µm in undoped sample, Grandjean texture (Fig. 3(a)) was observed where the chiral nematic director is confined parallel to the glass plate in multi-domains. At 6 V/µm, the helical axes of CLC molecules completely aligned along the direction of applied electric field and perpendicular to the substrate. Therefore dark homeotropic state appears (Fig. 3(b)) under crossed polarizers. The threshold voltage of these samples depends upon the cell thickness (d), pitch (p), chiral concentration (C), dielectric anisotropy ($\Delta\varepsilon$) and helical twisting power (HTP) as described by well known Eq. (10):

$$E = V/d = \frac{\pi^2}{p} C \sqrt{\frac{k_{22}}{\varepsilon_0 \Delta\varepsilon}} = \pi^2 .HTP.C. \sqrt{\frac{k_{22}}{\varepsilon_0 \Delta\varepsilon}} \quad \ldots (10)$$

whereas in case of doped SWCNT samples, the observed electro-optic switching behavior was predicted to analogous with undoped samples under the restriction of SWCNT network. The optical texture (Fig. 3(c)) of SWCNT doped CLC shows that SWCNTs affects the morphological response in 'Switch OFF' state (0 V/µm). At E=4.8 V/µm, the unwinding of helical structure takes place and the network of SWCNT clearly visible under crossed polarizers (Fig. 3(d)). The brightest lines in the homeotropic texture signatures the distribution of SWCNTs network due to anisotropic coupling of SWCNT with chiral doped nematic liquid crystals. Figure 4 clearly provides the hypothetical modeling for the electro optic switching in the corresponding optical textures (Fig. 3) of undoped and 0.4 wt% SWCNT's doped CLC samples. When an electric field is applied, the molecules trigger electrically from 'Switch OFF' to 'Switch ON State'[23]. The liquid crystal molecules aligned perfectly perpendicular to the glass substrate along the direction of applied electric field and the SWCNT's network is clearly visible in this state over the transparent ITO substrate in the SWCNT doped CLC sample when viewed under optical polarizing microscope.

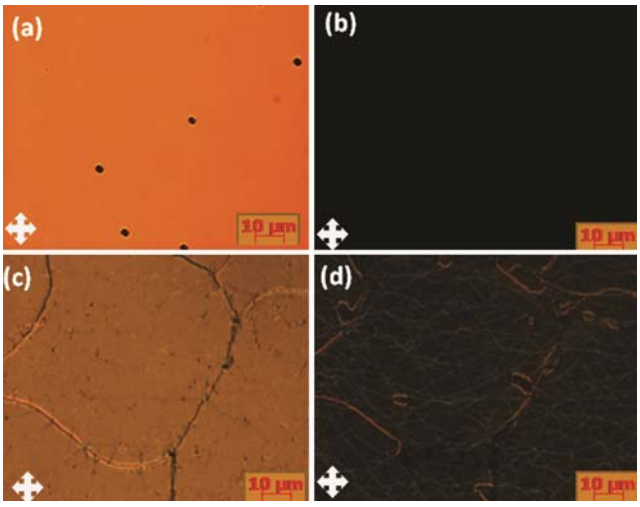

Fig. 3 — Polarized optical microscopy textures of (a) switch off state, (b) switch on state of undoped sample, (c) switch off state and (d) switch on state of SWCNT's doped CLC sample.

We believe that the interaction between surface anchoring, CLC molecules and π–π electron stacking contributes to the ac conductivity of the CNT doped samples. Therefore, ac conductivity σ_{ac} of all samples are calculated by using experimental data of the imaginary part of the complex permittivity (ε''), which was calculated by recording capacitance in the frequency range 50 Hz to 1 MHz by using LCR meter (Model Fluke). Hence ac conductivity can be computed experimentally by relation:

$$\sigma_{ac} = \varepsilon_0 \varepsilon'' \omega \quad \ldots (11)$$

where, ε_0 is permittivity of the free space, ε'' is the imaginary part of permittivity (recorded experimentally) and ω is the angular frequency. Figure 5 clearly hints the enhancement in conductivity at the interface formation by CNTs in liquid crystal matrix which contributes to the electrical response of the doped material. Also an increase in the conductivity normally associated with the capacitor character of the liquid crystal cell. This highest concentrated sample of SWCNT (0.4 wt%) doped CLC is probably very close to percolation with SWCNT clusters present. These aggregates in the cell can act as an array of capacitors and hence enhancement in the AC conductivity was predicted. These experimental results were again revivified with the help of theoretical modeling of electrical conductivity of these SWCNT doped CLC sample by using artificial neural network approach.

For this, we have used six training functions (TRAINGDX, TRAINGDA, TRAINGD, TRAINCGB, TRAINOSS, and TRAINLM) and feedforward backpropagation (FFBP) network is used for mapping between inputs and output patterns. A three-layer feedforward network is created for the prediction of effective electrical conductivity of SWCNT's doped samples over a wide concentration of dispersed phase of SWCNT in CLC between 0 to 0.40 wt%.

The effective electrical conductivity of SWCNT's doped chiral nematic composites as filler SWCNT's (wt%) is plotted in Fig. 5 with concentration of dispersed phase (filler) over the range between 0 to 0.40 wt%. It is observed that effective electrical conductivity of these composites get enhanced by the addition of SWCNT's. The maximum value of effective electrical conductivity 6.8595 $\Omega^{-1}cm^{-1}$ (TRAINOSS) are achieved for SWCNT's doped chiral nematic LC composites. The enhancement in the effective electrical conductivity of these composites is expected, as the electrical conductivity of the SWCNT is significantly higher than that of chiral nematic system.

Figure 6 depicts the comparison of experimental and predicted values of effective electrical conductivity of different SWCNT's doped chiral nematic LC composites by using different training functions. All

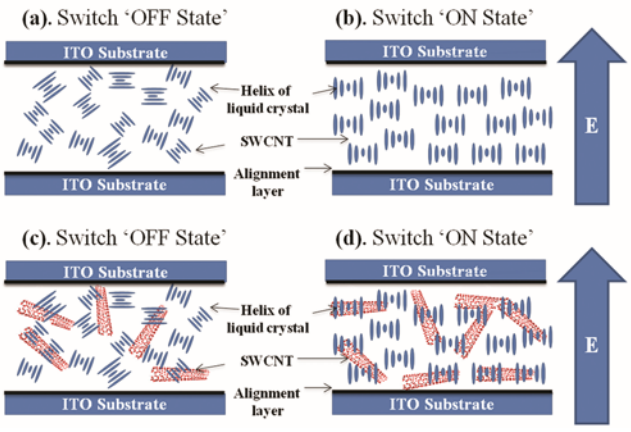

Fig. 4 — Hypothetical model of electro-optic switching (a) switch off state, (b) switch on state of undoped sample, (c) switch off state and (d) switch on state of SWCNT's doped CLC sample.

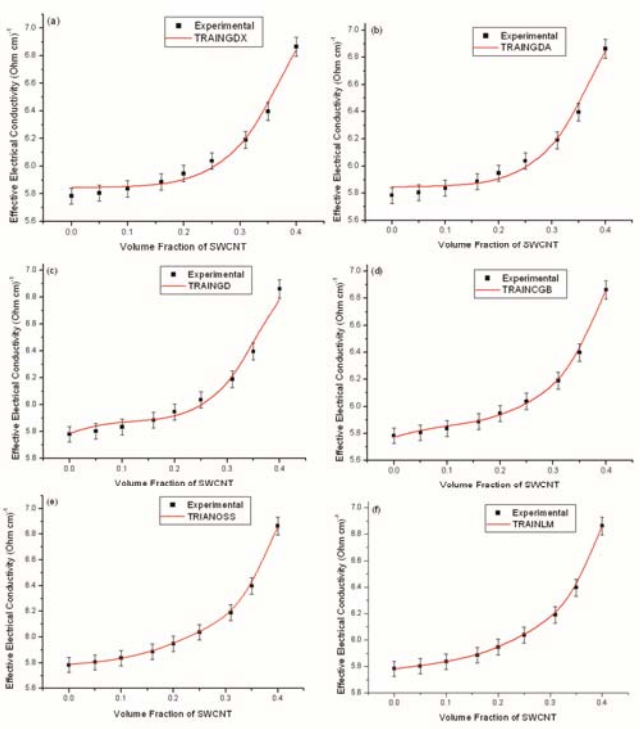

Fig. 5 — Comparison of experimental and theoretical results of electrical conductivity of SWCNT's doped chiral nematic liquid crystals by using artificial neural networks with trained function (a) TRAINGDX, (b) TRAINGDA, (c) TRAINGD, (d) TRAINCGB, (e) TRAINOSS and (f) TRAINLM.

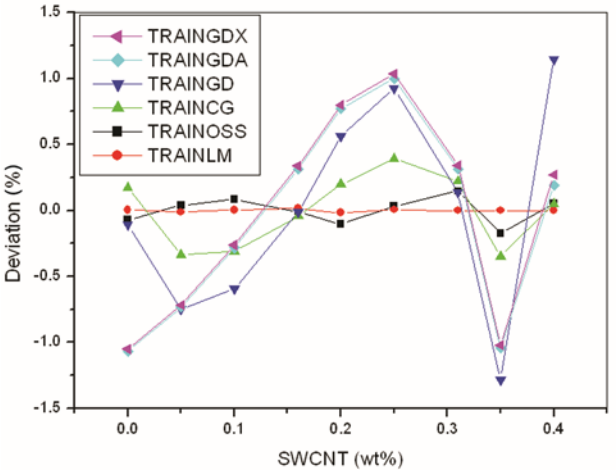

Fig. 6 — % deviation in electrical conductivity of SWNCT doped CLC samples as predicted by using different trained functions.

Table 1 — Mean square error (MSE) of different training functions

Training functions	Mean square error (MSE)
TRAINCGB	0.000246009
TRAINGD	0.0022579
TRAINGDA	0.00191767
TRAINGDX	0.00188113
TRAINLM	3.12617×10^{-7}
TRAINOSS	3.40434×10^{-5}

the predictions of FFBP, results of all the training functions TRAINCGB, TRAINLM, and TRAINOSS are close to each other and also closely match with the experimental results. As it is clear that all the training functions are based on feedforward backpropagation, therefore, slight variation in effective electrical conductivity is observed. Better results are obtained and the average percentage deviation (Table 1) is least if we use TRAINLM as training function in all the SWCNT doped CLC composites. Figure 7 shows regression plot which support the data in Fig. 6. In case of TRAINGD, maximum epoch has been reached (Fig. 7(f)) during training algorithms run at the uniform threshold transfer functions- Tangent sigmoid (TANSIG) and pure linear (PURELIN) for 1000 epochs. Hence performance and goal were not met the required condition whereas in another case it can be achieved successfuly.

5 Conclusions

We have sucessfully investigated the electrical switch behavior of SWCNT's doped CLC samples. The coupling between LC molecules and CNT's created a promising novel electrical properties aiming at the invention of novel soft materials at the molecular

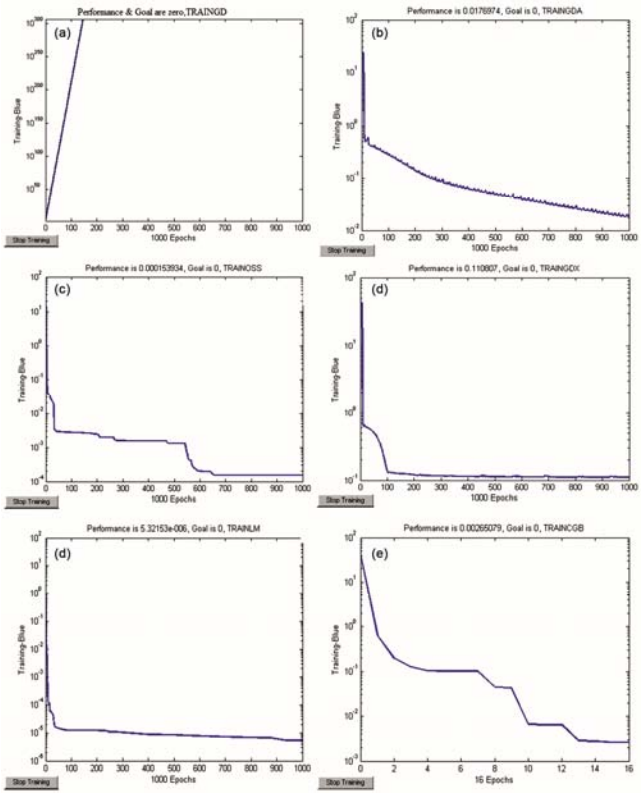

Fig. 7 — Regression plot (a) TRAINGD, (b) TRAINGDA, (c) TRAINOSS, (d) TRAINGDX, (e) TRAINLM and (f) TRAINCGB.

level. Our experimental results show the simplest agreement with the theoretical modeling of electrical conductivity by using artificial neural network approach. It's ended that completely different training functions of artificial neural networks exhibit the potential to predict electrical conductivity of SWCNT's doped CLC materials which might have potential applications in liquid crystal display technology. The interest of this work is additionaly self addressed to liquid crystal device wherever trade demands high electrical conductivity. Hence it claims that different models of ANN can be used to predict the effective electrical conductivity of these complex liquid crystal structures composites.

References

1 Chang C K, Chiu S W, Kuo H L & Tang K T, *Appl Phys Lett*, 100 (2012) 043501.
2 Lim Y J, Bhattacharyya S S, Tie W, Park H R, Lee Y H & Lee S H, *Liq Cryst*, 40 (2013) 1202.
3 Trushkevych O, *J Phys D: Appl Phys*, 41 (2008) 125106.
4 Joshi T, Kumar A, Prakash J & Biradar A M, *Liq Cryst*, 37 (2010) 1433.
5 Zhang Z & Friedrich K, *Compos Sci Technol*, 63 (2003) 2029.

6 Qi H & Hegmann T, *J Mater Chem*, 18 (2008) 3288.
7 Kumar R & Raina K K, *Liq Cryst*, 42 (2015) 119.
8 Kumar R & Raina K K, *Liq Cryst*, 41 (2014) 694.
9 Middha M, Kumar R & Raina K K, *Ferroelectrics*, 495 (2016) 75.
10 Joshi T, *J Phys D: Appl Phys*, 44 (2011) 315404.
11 Kumar R & Raina K K, *Liq Cryst*, 11 (2016) 1.
12 Dolgov L, Yaroshchuk O & Lebovka M, *Mole Cryst Liq Cryst*, 496 (2008) 212.
13 Middha M, Kumar R & Raina K K, *Liq Cryst*, 42 (2015) 1028.
14 Dolgov L, Yaroshchuk O, Tomylko S & Lebovka N, *Condens Matter Phys*, 15 (2012) 1.
15 Therdthai N & Zhou W, *J Food Eng*, 50 (2001) 107.
16 Hezave A Z, Lashkarbolooki M & Raeissi S, *Fluid Phase Equilib*, 314 (2012) 128.
17 Singh R, Bhoopal R S & Kumar S, *Build Environ*, 6 (2011) 2603.
18 Jalali-Heravi M & Fatemi M H, *J Chromatogr A*, 897 (2000) 227.
19 Kurt H & Kayfeci M, *Appl Energy*, 86 (2009) 2244.
20 Esfe M H, Seyfolah S, Mehdi B, Davood T Omid M & Somchai W, *J Therm Anal Calorim*, 118 (2014) 287.
21 Heristev R M, *The artificial neural network book*, (GNU Public License), 1998.
22 Williams D R & Hinton G E, *Nature*, 323 (1986) 533.
23 Kumar R & Raina K K, *AIP Conf Proc*, 1393 (2011) 46.